

# One-dimensional polyhedral chain of ThCl<sub>6</sub> encapsulated within single-walled carbon nanotubes

Kuganathan, K.

Published PDF deposited in Coventry University's Repository

**Original citation:**

[Kuganathan, K 2021, 'One-dimensional polyhedral chain of ThCl<sub>6</sub> encapsulated within single-walled carbon nanotubes', AIP Advances, vol. 11, 065117.

<https://dx.doi.org/10.1063/5.0051200>

DOI 10.1063/5.0051200

ESSN 2158-3226

Publisher: American Institute of Physics

**All article content, except where otherwise noted, is licensed under a Creative Commons Attribution (CC BY) license.**

# One-dimensional polyhedral chain of $\text{ThCl}_6$ encapsulated within single-walled carbon nanotubes

Cite as: AIP Advances **11**, 065117 (2021); <https://doi.org/10.1063/5.0051200>

Submitted: 23 March 2021 . Accepted: 28 May 2021 . Published Online: 09 June 2021

 Navaratnarajah Kuganathan



View Online



Export Citation



CrossMark

## ARTICLES YOU MAY BE INTERESTED IN

[Defect and dopant properties in  \$\text{CaMnO}\_3\$](#)

AIP Advances **11**, 055106 (2021); <https://doi.org/10.1063/5.0048401>

[Printed flexible supercapacitor: Ink formulation, printable electrode materials and applications](#)

Applied Physics Reviews **8**, 021319 (2021); <https://doi.org/10.1063/5.0048446>

[Impact of oxygen on gallium doped germanium](#)

AIP Advances **11**, 065122 (2021); <https://doi.org/10.1063/5.0054643>

Call For Papers!

AIP Advances

**SPECIAL TOPIC:** Advances in  
Low Dimensional and 2D Materials

# One-dimensional polyhedral chain of $\text{ThCl}_6$ encapsulated within single-walled carbon nanotubes

Cite as: AIP Advances 11, 065117 (2021); doi: 10.1063/5.0051200

Submitted: 23 March 2021 • Accepted: 28 May 2021 •

Published Online: 9 June 2021



View Online



Export Citation



CrossMark

Navaratnarajah Kuganathan<sup>a)</sup> 

## AFFILIATIONS

Department of Materials, Imperial College London, London SW7 2AZ, United Kingdom and Faculty of Engineering, Environment and Computing, Coventry University, Priory Street, Coventry CV15FB, United Kingdom

<sup>a)</sup> Author to whom correspondence should be addressed: [n.kuganathan@imperial.ac.uk](mailto:n.kuganathan@imperial.ac.uk)

## ABSTRACT

Using density functional theory together with dispersion correction, we optimize geometries and calculate encapsulation energies, charge transfer, and electronic structures of a one-dimensional  $\text{ThCl}_6$  chain encapsulated within single-walled carbon nanotubes. The optimized structures are in agreement with the experimentally observed single chain of  $\text{ThCl}_6$  confined within nanotubes. Exoergic encapsulation energies indicate that the chain is thermodynamically stable inside the nanotubes. The inclusion of dispersion correction enhanced the encapsulation. The strong nature of encapsulation is further confirmed by the charge transfer between the nanotubes and the chain. The one-dimensional chain structure exhibits a small increase (0.20 eV) in the bandgap compared to that of bulk  $\text{ThCl}_4$ . The metallic (15,0) tube becomes a narrow gap semiconductor upon encapsulation, while the semiconducting nature of the (17,0) tube is still kept despite the reduction in the bandgap.

© 2021 Author(s). All article content, except where otherwise noted, is licensed under a Creative Commons Attribution (CC BY) license (<http://creativecommons.org/licenses/by/4.0/>). <https://doi.org/10.1063/5.0051200>

## I. INTRODUCTION

Single-walled nanotubes (SWNTs) are of great interest for their ability to encapsulate a variety of one-dimensional (1D) inorganic nanocrystals.<sup>1–6</sup> The synthesis of SWNTs filled with inorganic nanocrystals has been considered as a possible route for studying the properties of low-dimensional materials and tuning the electronic properties of nanotubes.<sup>7–10</sup> Much experimental work has been reported on the synthesis and characterization of metal halides and metal chalcogenides encapsulated within SWNTs.<sup>4,5,7,11–14</sup> In general, encapsulation resulted in a change in the encapsulated material relative to its bulk. A high resolution transmission electron microscopy (HRTEM) study on the filling of KI resulted in the formation of 1D  $2 \times 2$  KI crystals in which both K and I form a 4:4 coordination in contrast to the 6:6 coordination observed in the bulk KI.<sup>1</sup> A similar low-dimensional structure with 4:4 coordination has also been observed in the experimental study of filling SWNTs with SnSe.<sup>15</sup> A unique 1D tubular structure of HgTe inside SWNTs was characterized by Carter *et al.*<sup>7</sup> upon the filling of molten HgTe.

In this tubular structure, both Hg and Te form three-dimensional coordination in contrast to the tetrahedral coordination observed for both He and Te in the bulk HgTe zinc blende structure.

In another experimental study, Sloan *et al.*<sup>2</sup> filled SWNTs with  $\text{ThCl}_4$  and recorded their images using HRTEM. The encapsulated structure is observed to be a one-dimensional chain consisting of  $\text{ThCl}_6$  polyhedral units along the tube axis and the diameter of the tube was reported to be 1.1 nm.<sup>2</sup> Furthermore, the polyhedral units are eight-coordinate and share their edges as observed in the bulk  $\text{ThCl}_4$ . The encapsulation of  $\text{ThCl}_4$  within SWNTs can be an ideal route to store Th as SWNT walls can provide protection from the chemical environment and external interactions.

Computational modeling techniques have been supportive in validating the experimentally observed structures within SWNTs and predicting the structural and electronic properties of the resultant encapsulated structures.<sup>16–18</sup> Significant effort has been devoted to study one-dimensional nanocrystals encapsulated within SWNTs theoretically.<sup>19–21</sup> Density functional theory (DFT)

simulations have been performed to validate the structures of 1D inorganic crystals, such as KI,<sup>17</sup> HgTe,<sup>22</sup> PbI<sub>2</sub>,<sup>23</sup> and SnSe,<sup>10</sup> encapsulated within SWNTs and study the electronic properties of the composites formed. In some simulation work, model structures have been proposed for crystals such as Cu<sup>24</sup> and CdTe<sup>18</sup> as lighter atoms are generally challenging to elucidate from HRTEM experiments.

In this study, we use spin-polarized mode DFT simulations to validate the experimentally observed 1D ThCl<sub>6</sub> chain confined within SWNTs and determine the nature of the interaction between the tube and chain. Furthermore, simulations enabled us to calculate the charge transferred between the guest and the host and electronic nature of the resultant composite relative to that of pristine SWNT.

## II. COMPUTATIONAL METHODS

All calculations were performed using spin-polarized mode of DFT as implemented in the VASP (Vienna *Ab initio* simulation package) code.<sup>25</sup> The exchange–correlation term was modeled using the generalized gradient approximation (GGA) parameterized by Perdew, Burke, and Ernzerhof (PBE).<sup>26</sup> The valence electronic configurations for C, Th, and Cl were 2s<sup>2</sup> 2p<sup>2</sup>, 6s<sup>2</sup> 6p<sup>6</sup> 6d<sup>2</sup> 7s<sup>2</sup>, and 3s<sup>2</sup> 3p<sup>5</sup>, respectively. The standard projected augmented wave (PAW) potentials<sup>27</sup> and a plane-wave basis set with a cutoff of 500 eV were employed. We used an 8 × 8 × 8 Monkhorst–Pack<sup>28</sup> *k*-point mesh for the bulk ThCl<sub>4</sub> structure. For the isolated 1D ThCl<sub>6</sub> chain structure and its structure encapsulated within SWNTs, a 4 × 1 × 1 Monkhorst–Pack *k*-point mesh was used. Structure optimizations were carried out using a conjugate gradient algorithm,<sup>29</sup> and the Hellman–Feynman theorem with Pulay corrections was used to obtain the forces on the atoms. In all relaxed structures, forces on the atoms were smaller than 0.01 eV/Å. We have included zero damping DFT-D3 dispersion correction as implemented by Grimme *et al.*<sup>30</sup>

For calculations on the infinite 1D ThCl<sub>6</sub> chain and ThCl<sub>6</sub>@SWNTs, periodic boundary conditions were applied to enforce a minimum lateral separation of 25 Å between structures in adjacent unit cells.

The encapsulation energy of the ThCl<sub>6</sub> chain can be calculated by considering the difference in the total energy of the ThCl<sub>6</sub>@SWNT and the total energies calculated for an isolated ThCl<sub>6</sub> chain structure and an isolated SWNT,

$$E_{enc} = E_{\text{ThCl}_6@\text{SWNT}} - E_{\text{SWNT}} - E_{\text{ThCl}_6}, \quad (1)$$

where  $E_{\text{ThCl}_6@\text{SWNT}}$  is the total energy of ThCl<sub>6</sub> encapsulated within a SWNT and  $E_{\text{SWNT}}$  and  $E_{\text{ThCl}_6}$  are the total energies of a SWNT and an isolated gas phase ThCl<sub>6</sub> chain, respectively.

Initial configurations, optimized geometries, and charge density plots were visualized using a 3D visualization program VESTA (Visualization for Electronic and Structural Analysis).<sup>31</sup> Density of state (DOS) plots were visualized and analyzed using XMGRACE software.<sup>32</sup> Bader charge analysis<sup>33</sup> enabled us to calculate the charge transferred between the nanotubes and the 1D ThCl<sub>6</sub> crystal. In this method, electronic charges on individual atoms in the relaxed configurations are calculated based on the partitioning method as implemented by Bader.<sup>33</sup>

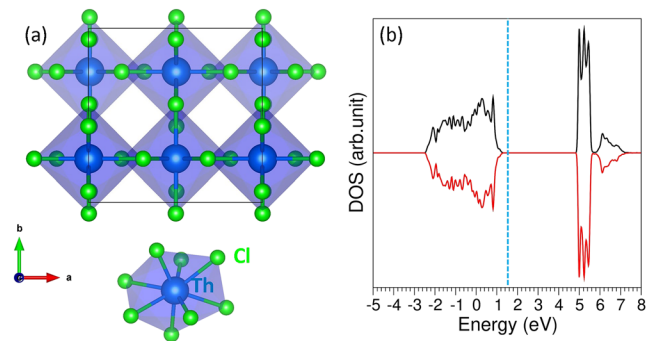


FIG. 1. (a) Crystal structure of ThCl<sub>4</sub> and (b) its total density of states plot.

## III. RESULTS AND DISCUSSION

### A. Crystal structure of ThCl<sub>4</sub>

ThCl<sub>4</sub> crystallizes in the tetragonal  $I4_1/amd$  space group. Its experimental lattice parameters measured at room temperature are reported to be  $a = b = 8.486$ ,  $c = 7.465$  Å, and  $\alpha = \beta = \gamma = 90^\circ$ .<sup>34</sup> Figure 1(a) shows its crystal structure in which each Th atom forms eightfold coordination with adjacent eight Cl atoms. The dodecahedron units formed by each Th are connected by their edges. There are two sets of Th–Cl bond distances [2.718 (4×) and 2.903 (4×)] present in each dodecahedron unit. In order to assess the quality of the pseudopotentials and basis sets used for C, Th, and Cl, we performed the full geometry optimization calculation on the crystal structure of ThCl<sub>4</sub> by relaxing positions of both atoms and the simulation box simultaneously. There is excellent agreement between the calculated and experimental values showing the efficacy of the simulation parameters in this study (see Table I). The DOS plot shows that the bulk ThCl<sub>4</sub> is a wide-gap semiconductor with a bandgap of 3.60 eV [see Fig. 1(b)].

### B. 1D ThCl<sub>6</sub> chain structure

Next, we considered the optimization of the 1D chain structure of ThCl<sub>6</sub> with periodic boundary conditions in the absence of a confining tube. This chain structure consisted of four ThCl<sub>6</sub> units (Th<sub>4</sub>Cl<sub>24</sub>) in the supercell with dimensions of  $16.97 \times 25 \times 25$  Å<sup>3</sup>. The relaxed structure is depicted in Fig. 2(a). Table II reports the calculated bond distances, bond angles, and the bandgap. The optimized structure resembles the starting configuration. The

TABLE I. Calculated and experimental lattice constants of the ThCl<sub>4</sub> crystal structure.

Parameter	Calculated	Experiment <sup>34</sup>	$ \Delta $ (%)
<i>a</i> (Å)	8.527	8.486	0.48
<i>b</i> (Å)	8.524	8.486	0.45
<i>c</i> (Å)	7.516	7.465	0.68
$\alpha = \beta = \gamma$ (deg)	90.0	90.0	0.00
Th–Cl (Å)	2.723/2.925	2.718/2.903	0.18/0.76
<i>V</i> (Å <sup>3</sup> )	546.32	537.57	1.63

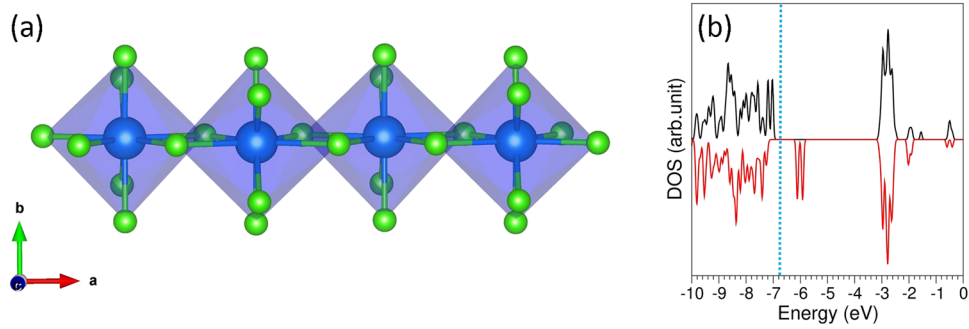


FIG. 2. (a) Relaxed structure of the 1D chain of  $\text{ThCl}_6$  with periodic boundary conditions and (b) its total DOS plot.

TABLE II. Calculated bond distances, bond angles, and bandgap of the 1D  $\text{ThCl}_4$  crystal structure. The corresponding values calculated for the bulk  $\text{ThCl}_4$  are also provided for comparison.

Property	Bulk	1d $\text{ThCl}_6$ chain
Th–Cl (Å)	2.718/2.903	2.760, 2.788/2.804, 2.818
Th–Cl–Th (deg)	111.05, 111.09	109.02, 109.08
Cl–Th–Cl (deg)	66.28, 68.95, 79.92, 92.51/155.82	56.41, 70.95, 85.68, 91.69/147.6
Bandgap (eV)	3.60	3.80

Th–Cl bond distances in the relaxed 1D chain deviate maximum by 0.1 Å. The bond angles slightly deviate from the values calculated for the bulk  $\text{ThCl}_4$ . The deviation in the structural parameters can be attributed to the discontinuation of Th–Cl bonds present in the 1D chain in contrast to those observed in the bulk  $\text{ThCl}_4$ .

As discussed earlier, bulk  $\text{ThCl}_4$  is a wide-bandgap semiconductor. The DOS of an infinite  $\text{ThCl}_6$  chain outside the tube is slightly distorted compared to that of bulk  $\text{ThCl}_4$ . In particular, the alpha/beta (spin up/spin down) states are different. This is because some Cl atoms exhibit single coordination with adjacent Th atoms in contrast to what observed in bulk  $\text{ThCl}_4$  [see Fig. 2(a)]. The bandgap for the 1D system (3.80 eV) is slightly larger than that calculated for the bulk (3.60 eV).

### C. Calculations on $\text{ThCl}_6$ @SWNT

Finally, we considered the modeling of 1D  $\text{ThCl}_6$  encapsulated within SWNTs. Three different sizes of SWNTs were selected. They are (15,0), (16,0), and (17,0) with diameters of 11.85, 12.54, and 13.53 Å, respectively. The selection of the (15,0) tube is due to its diameter close to the value (11.00 Å) reported in the experiment.<sup>2</sup> In addition, we also considered two other tubes with larger diameters of 13.53 Å to look at the confinement effect of the diameter. A supercell comprising four  $\text{ThCl}_6$  units (supercell length = 16.97 Å) and an (n,0) SWNT (n = 15, 16, and 17) comprising four unit cells (supercell length = 17.01 Å) were very close to each other. The number of carbon atoms in the pristine (15,0), (16,0), and (17,0) SWNTs is 240, 256, and 268, respectively. We applied periodic boundary conditions

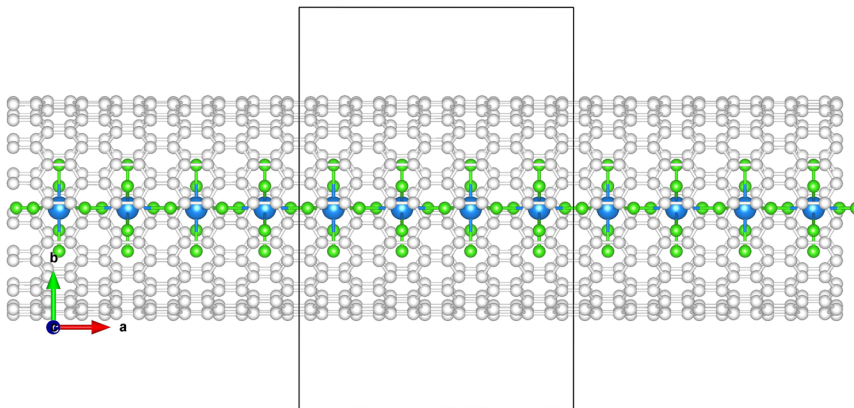


FIG. 3. Structure of the infinite  $\text{ThCl}_6$  chain inside an infinite SWNT. The box in this structure indicates the supercell with periodic boundary conditions.

**TABLE III.** Calculated encapsulation energies, bond lengths, bond angles, and charge transferred between the SWNT and the ThCl<sub>6</sub> chain.

	$dt$ (Å)	$E_{\text{enc}}$ (eV)/ ThCl <sub>6</sub> unit	Th-Cl (Å)	Th-Cl-Th (deg)	Cl-Th-Cl (deg)	C-Cl (deg)	Charge ( $ e $ )/ ThCl <sub>6</sub> unit
Dispersion							
ThCl <sub>6</sub> @(15,0)	11.85	-3.01	2.71, 2.79/2.85, 2.87	107.29, 107.35	57.08, 71.09, 72.74, 92.69/141.73, 145.62	3.25, 3.27, 3.30, 3.48	-0.93
ThCl <sub>6</sub> @(16,0)	12.54	-3.06	2.72, 2.78/2.82, 2.89	107.30, 107.36	58.09, 68.32, 70.34/142.67, 145.78	3.26, 3.34, 3.45, 3.50,	-0.95
ThCl <sub>6</sub> @(17,0)	13.53	-3.13	2.71, 2.79/2.85, 2.90	107.29, 107.35	56.66, 68.98, 82.27, 90.5/143.26, 145.59	3.30, 3.37, 3.47	-0.92
Non-dispersion							
ThCl <sub>6</sub> @(15,0)	11.85	-1.54	2.74, 2.77/2.84, 2.90	106.24, 106.39	60.03, 73.14, 75.46, 80.98/130.98, 143.45	3.33, 3.45, 3.56	-0.89
ThCl <sub>6</sub> @(16,0)	12.54	-1.89	2.76, 2.78/2.83, 2.87	107.34, 109.59	61.03, 72.14, 74.46, 81.98/132.98, 145.45	3.36, 3.43, 3.46	-0.89
ThCl <sub>6</sub> @(17,0)	13.53	-2.14	2.75, 2.79/2.86, 2.93	108.23, 109.06	59.65, 60.34, 85.34, 91.23/146.56, 147.45	3.39, 3.45, 3.56	-0.90

to supercells of Th<sub>4</sub>Cl<sub>24</sub>@(n,0) in order to model the entire supercell (SWNT+ThCl<sub>6</sub>) as an infinite system. Figure 3 shows the modeled ThCl<sub>6</sub> chain encapsulated within a SWNT.

The values calculated for the bond distances and bond angles deviate slightly from the values calculated for the gas phase 1d infinite ThCl<sub>6</sub> chain (see Table III), indicating a small distortion in

the crystal upon encapsulation. In all cases, encapsulation energies are negative, meaning that they are thermodynamically stable inside the tube. For the smaller tube, the encapsulation energy is less exothermic due to a small distortion. Encapsulation energies were calculated without dispersion correction to look at the contribution of short-range van der Waals forces. Calculations clearly show

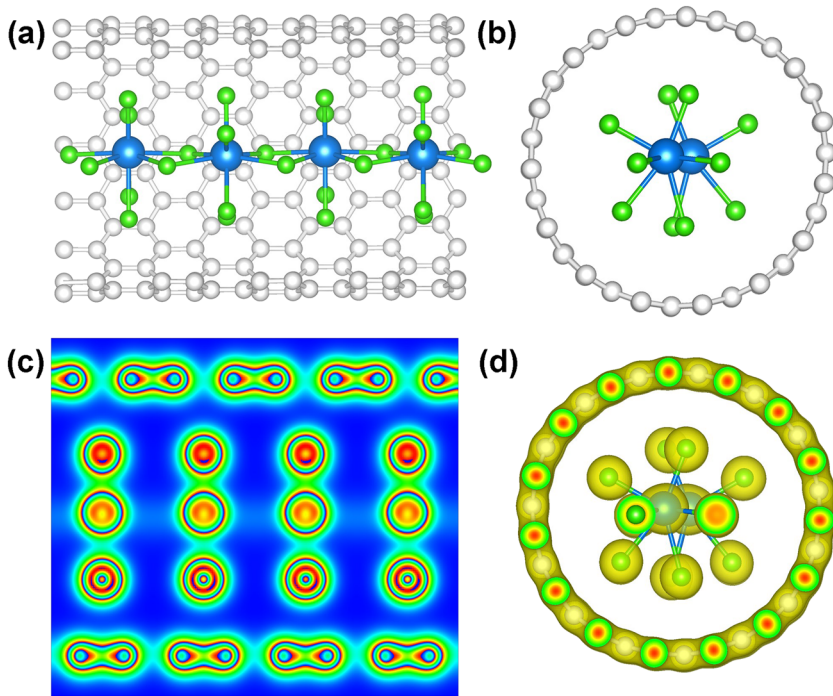


**FIG. 4.** (a) Relaxed structure of an infinite ThCl<sub>6</sub> chain inside an infinite (15,0) tube, (b) its cross-sectional view, (c) charge density plot showing the interaction between the tube and the chain, and (d) its cross-sectional view.

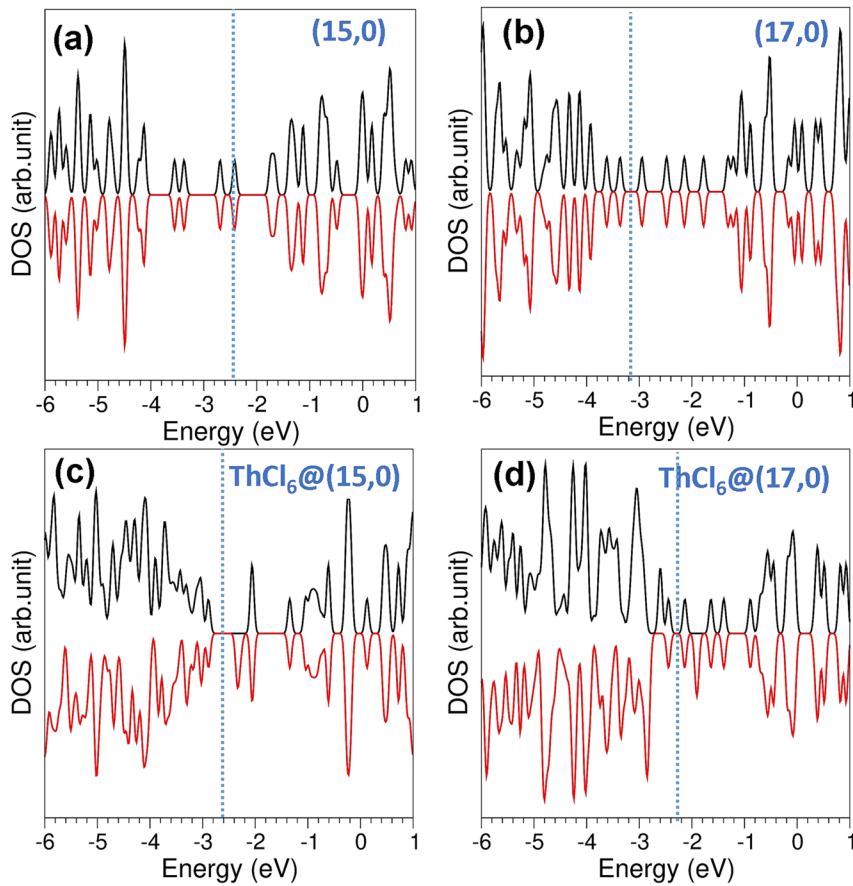


**FIG. 5.** DOS plots of (a) pristine (15,0) tube, (b) pristine (17,0), (c) ThCl<sub>6</sub>@(15,0), and (d) ThCl<sub>6</sub>@(17,0).

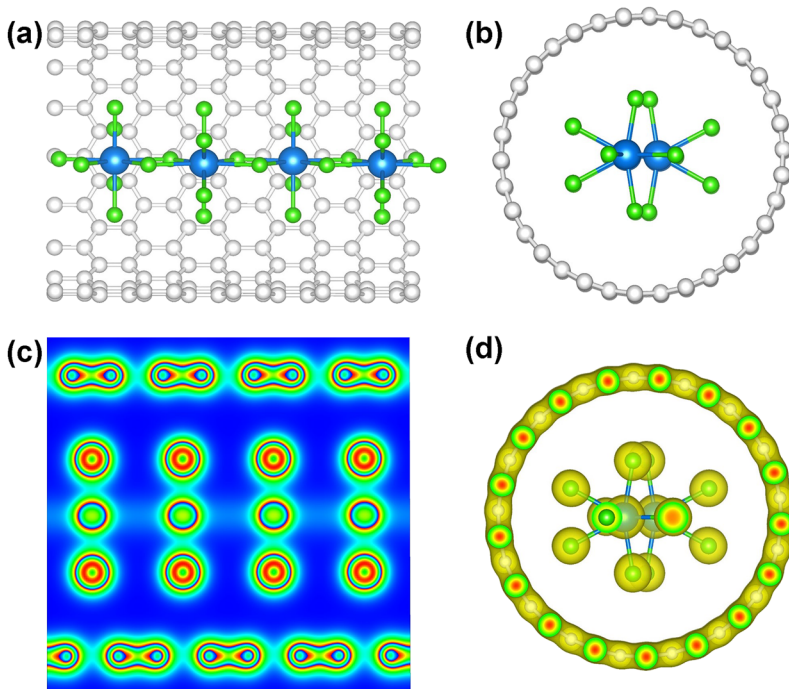


**FIG. 6.** (a) Relaxed structure of an infinite ThCl<sub>6</sub> chain inside an infinite (17,0) tube, (b) its cross-sectional view, (c) charge density plot showing the interaction between the tube and the chain, and (d) its cross-sectional view.

that dispersion correction improves the encapsulation energies. The bond distances, bond angles, and the amount of charges are not significantly affected by the dispersion correction. Figure 4 shows the relaxed structure of  $\text{ThCl}_6@(\text{15},0)$  and charge density of the composite. The distortion is further confirmed by the charge density plot in Fig. 4(d). The (15,0) tube is metallic [see Fig. 5(a)]. Upon encapsulation, the tube becomes a narrow gap semiconductor. This can be due to the charge transfer from the tube to the chain. The semiconducting nature (17,0) tube is still kept upon encapsulation though there is a small reduction in the bandgap [see Figs. 5(b) and 5(d)]. The relaxed structure of  $\text{ThCl}_6@(\text{17},0)$  together with its charge density plot is shown in Fig. 6. A small distortion is observed as evidenced by the charge density plot [see Fig. 6(d)]. The Bader charge analysis shows that there is a charge of  $\sim 1 |e|$  transferred from the tube to the chain, meaning that the  $\text{ThCl}_6$  chain prefers to form an anion. The calculated C–Cl bond distances (3.25–3.48 Å) confirm that there is a non-covalent interaction between the tube and the chain. This is further confirmed by the charge density plots (see Figs. 4 and 5).

#### IV. CONCLUSIONS

In conclusion, the encapsulation of the one-dimensional  $\text{ThCl}_6$  chain within different sizes of SWNTs was studied using density functional theory with dispersion correction. The calculated structures are in good agreement with the structure observed in the HRTEM experiment. The encapsulation energies are exoergic, meaning that the chain structure inside SWNTs is thermodynamically stable. This is evidenced by the charge transfer between SWNTs and the chain. The inclusion of dispersion correction improved the encapsulation. There is a small reduction in the bandgap in the  $\text{ThCl}_6$  chain compared to its bulk structure. Encapsulation introduces a gap in the metallic (15,0) tube, whereas the semiconducting nature of the (17,0) tube is retained though there is a reduction in the bandgap upon encapsulation.

#### ACKNOWLEDGMENTS

Professor Robin W. Grimes is acknowledged for useful discussions. Computational facilities and support were provided by the High Performance Computing Centre at Imperial College London.

The authors declare that there is no competing financial interest.

#### DATA AVAILABILITY

The data that support the findings of this study are available from the corresponding author upon reasonable request.

#### REFERENCES

- 1 J. Sloan *et al.*, *Chem. Phys. Lett.* **329**, 61 (2000).
- 2 J. Sloan, A. I. Kirkland, J. L. Hutchison, and M. L. H. Green, *Chem. Commun.* **2002**, 1319.
- 3 E. Philp, J. Sloan, A. I. Kirkland, R. R. Meyer, S. Friedrichs, J. L. Hutchison, and M. L. H. Green, *Nat. Mater.* **2**, 788 (2003).
- 4 E. Flahaut, J. Sloan, S. Friedrichs, A. I. Kirkland, K. S. Coleman, V. C. Williams, N. Hanson, J. L. Hutchison, and M. L. H. Green, *Chem. Mater.* **18**, 2059 (2006).
- 5 J. Sloan, A. I. Kirkland, J. L. Hutchison, and M. L. H. Green, *Acc. Chem. Res.* **35**, 1054 (2002).
- 6 A. Vasylenko, S. Marks, J. M. Wynn, P. V. C. Medeiros, Q. M. Ramasse, A. J. Morris, J. Sloan, and D. Quigley, *ACS Nano* **12**, 6023 (2018).
- 7 R. Carter *et al.*, *Phys. Rev. Lett.* **96**, 215501 (2006).
- 8 L. J. Li, T. W. Lin, J. Doig, I. B. Mortimer, J. G. Wiltshire, R. A. Taylor, J. Sloan, M. L. H. Green, and R. J. Nicholas, *AIP Conf. Proc.* **893**, 1047 (2007).
- 9 B. Cantor *et al.*, *Scr. Mater.* **44**, 2055 (2001).
- 10 R. Carter *et al.*, *Dalton Trans.* **43**, 7391 (2014).
- 11 N. A. Kiselev *et al.*, *J. Microsc.* **232**, 335 (2008).
- 12 A. A. Eliseev *et al.*, *Carbon* **48**, 2708 (2010).
- 13 C. Xu *et al.*, *Chem. Commun.* **2000**, 2427.
- 14 S. Friedrichs, R. R. Meyer, J. Sloan, A. I. Kirkland, J. L. Hutchison, and M. L. H. Green, *Chem. Commun.* **2001**, 929.
- 15 C. A. Slade, A. M. Sanchez, and J. Sloan, *Nano Lett.* **19**, 2979 (2019).
- 16 C. Yam, C. Ma, X. Wang, and G. Chen, *Appl. Phys. Lett.* **85**, 4484 (2004).
- 17 E. L. Sceats, J. C. Green, and S. Reich, *Phys. Rev. B* **73**, 125441 (2006).
- 18 N. Kuganathan and A. Chroneos, *Inorg. Chim. Acta* **488**, 246 (2019).
- 19 D. G. Calatayud *et al.*, *ChemistryOpen* **7**, 144 (2018).
- 20 M. Wilson, *Chem. Phys. Lett.* **366**, 504 (2002).
- 21 J. M. Wynn, P. V. C. Medeiros, A. Vasylenko, J. Sloan, D. Quigley, and A. J. Morris, *Phys. Rev. Mater.* **1**, 073001 (2017).
- 22 N. Kuganathan and J. C. Green, *Int. J. Quantum Chem.* **108**, 797 (2008).
- 23 N. Kuganathan and J. C. Green, *Int. J. Quantum Chem.* **109**, 171 (2009).
- 24 N. Kuganathan and J. C. Green, *Chem. Commun.* **2008**, 2432.
- 25 G. Kresse and J. Furthmüller, *Phys. Rev. B* **54**, 11169 (1996).
- 26 J. P. Perdew, K. Burke, and M. Ernzerhof, *Phys. Rev. Lett.* **77**, 3865 (1996).
- 27 P. E. Blöchl, *Phys. Rev. B* **50**, 17953 (1994).
- 28 H. J. Monkhorst and J. D. Pack, *Phys. Rev. B* **13**, 5188 (1976).
- 29 W. H. Press, S. A. Teukolsky, W. T. Vetterling, and B. P. Flannery, *Numerical Recipes in C: The Art of Scientific Computing*, 2nd ed. (Cambridge University Press, 1992).
- 30 S. Grimme, J. Antony, S. Ehrlich, and H. Krieg, *J. Chem. Phys.* **132**, 154104 (2010).
- 31 K. Momma and F. Izumi, *J. Appl. Crystallogr.* **41**, 653 (2008).
- 32 P. J. Turner, XMG-RACE, Version 5.1.19, Centre for Coastal and Land-Margin Research, Oregon Graduate Institute of Science and Technology, Beaverton, OR, 2005.
- 33 R. F. W. Bader, *Theor. Chem. Acc.* **105**, 276 (2001).
- 34 K. F. Mucker, G. S. Smith, Q. Johnson, and R. E. Elson, *Acta Crystallogr., Sect. B: Struct. Crystallogr. Cryst. Chem.* **25**, 2362 (1969).